Hindawi Publishing Corporation
Journal of Nanomaterials
Volume 2014, Article ID 837695, 7 pages
http://dx.doi.org/10.1155/2014/837695

Research Article

The Tissue Response and Degradation of Electrospun Poly(ε-caprolactone)/Poly(trimethylene-carbonate) Scaffold in Subcutaneous Space of Mice

Tao Jiang,[1,2] Guoquan Zhang,[1] Wentong He,[1] Hui Li,[1] and Xun Jin[1]

[1] *Department of Histology and Embryology, Logistics University of Chinese People's Armed Police Forces, Tianjin 300309, China*
[2] *Tianjin Key Laboratory of Cardiovascular Remodeling and Target Organ Injury, Tianjin 300162, China*

Correspondence should be addressed to Tao Jiang; jiangtao_wjhq@sina.com

Received 15 May 2014; Revised 8 August 2014; Accepted 16 August 2014; Published 3 September 2014

Academic Editor: Xingcai Wu

Due to the advantage of controllability on the mechanical property and the degradation rates, electrospun PCL/PTMC nanofibrous scaffold could be appropriate for vascular tissue engineering. However, the tissue response and degradation of electrospun PCL/PTMC scaffold in vivo have never been evaluated in detail. So, electrospun PCL/PTMC scaffolds with different blend ratios were prepared in this study. Mice subcutaneous implantation showed that the continuous degradation of PCL/PTMC scaffolds induced a lasted macrophage-mediated foreign body reaction, which could be in favor of the tissue regeneration in graft.

1. Introduction

Although there is a strong patient demand for small diameter (<6 mm) vascular bypass grafts every year, the development of an ideal replacement has been a daunting task with minimal success. The only clinically approved alternatives to autologous grafts for revascularization procedures are ePTFE and Dacron synthetic biostable prostheses, both have high failure rates for small diameter vessel replacements [1]. Over the last few years, a number of studies have been published on new vascular grafts based on PCL [2–5]. There are also a few reports about vascular grafts based on PTMC [6, 7]. Poly(ε-caprolactone) (PCL) and poly(trimethylene carbonate) (PTMC) are two aliphatic polyesters. They are both biodegradable and biocompatible but have different biodegradation rates and different mechanical resistance. PTMC degrades more rapidly than PCL in vivo, and the elasticity of PTMC is also better than PCL [8, 9]. The synthetic copolymer of the two, a trimethylene carbonate-co-ε-caprolactone polymer, has been investigated as biopolymer to be used for surgery and nerve guide repairs because of its high biocompatibility and the advantage of controllable both the mechanical property and the degradation rates [10]. The more promising electrospinning of PCL/PTMC nanofibrous scaffold also was reported [11]. However, the tissue response and degradation of electrospun PCL/PTMC scaffold in vivo have never been evaluated in detail. In order to develop a kind of novel biomaterial for vascular grafts, this study was to observe and understand the complex interactions between host response and PCL/PTMC scaffold material after subcutaneous implantation in mice.

2. Materials and Methods

2.1. Materials. PCL (Mw~80,000) and PTMC (Mw~100,000) were purchased from Daigang Biomaterial Co., Ltd. (Jinan, China). Dichloromethane (DCM) and N, N-dimethylformamide (DMF) were purchased from Tianjin Chemical Reagent Company and used as received. Monoclonal rat anti-mouse CD11b antibody was purchased from R&D Systems, Inc. (Minneapolis, USA). Monoclonal rat anti-mouse CD68 antibody was from BD Biosciences Pharmingen (BD Biosciences, San Jose, CA). Goat anti-rat IgG (secondary antibody) labeled with FITC (1 : 100) or Cy3 (1 : 200) was purchased from Gibco, Invitrogen (Carlsbad, CA). Phalloidin-TRITC and Hoechst 33342 were from

Sigma-Aldrich (St. Louis, MO, USA). Male Balb/c mice were purchased from the Laboratory Animal Center of the Academy of Military Medical Sciences (Beijing, China).

2.2. Fabrication of PCL/PTMC Scaffolds. PCL and different blend ratios of PCL and PTMC (3 : 1, 1 : 1, and 1 : 3 w/w) were dissolved in a mixture of DCM/DMF (3 : 1, v/v) to prepare the electrospinning solutions at a concentration of 10% [11]. The solutions were then carefully placed into 20 mL plastic syringe with an 18 gage blunt tip needle. Electrospinning was carried out under a fixed electric field of 20 kV/16 cm. The flow rate of the solutions was controlled at 4 mL/h by a single syringe pump. A rotating mandrel (2 mm diameter, stainless steel rod) was used as collector. The mandrel was removed yielding a tubular graft. All experiments were carried out at room temperature and a relative humidity of 40%. The resulting fibers were further dried for 24 h at room temperature in a vacuum drying oven to remove the residual organic solvent and moisture. The electrospun tubular grafts were examined by scanning electron microscopy (SEM) after sputtering the surface with gold. The molecular interactions of the blend electrospun fibers were assayed on a Fourier-transform infrared (FT-IR) spectrometer.

2.3. Animal Model. Twenty male BALB/c mice (aged 5-6 weeks, mice weighting 22–26 g) were divided into 4 groups (five in each group) randomly and then anesthetized by 0.4% (w/v) pentobarbital (4 mg/100 g). In PCL group, one PCL tubular scaffold (1.5 cm long, 2 mm inner diameter) was implanted in the dorsal subcutaneous space of Balb/c mice [12]. In PCL/PTMC (3 : 1), PCL/PTMC (1 : 1), and PCL/PTMC (1 : 3) group, same size tubular scaffolds were implanted, respectively. After implantation for 1 month, the animals were sacrificed, and the implant and surrounding tissue were isolated for histological analyses. All procedures were performed in accordance with the Health Guide for the Care and Use of Laboratory Animals of Logistics University of CAPF.

2.4. Histological Evaluation. Mice were killed at the indicated time point by cervical dislocation; the tubular grafts implanted under the skin were removed carefully and embedded in the tissue-Tek (OCT), followed by being quickly frozen with nitrogen liquid and stored at −80°C for use. Cryosections, 8 μm in thickness, were cut transversely with cryostat and collected on the glass slide coated with APES. After drying for 1 hour, sections were fixed with acetone for 30 min. To assess the tissue responses to tubular scaffold implants, some of these slides were stained with hematoxylin and eosin. To assess the extent of the inflammatory cells, immunofluorescence analyses were carried out on some slides. After washing with 0.01MPBS, specimens were blocked with 0.1% bovine serum albumin (BSA) for 1 h at room temperature. Subsequently, sections were treated with rat monoclonal anti-mouse CD11b and CD68 antibody at 4°C overnight, respectively. After rinsing, secondary antibody, cy3 labeled goat anti-rat IgG (Invitrogen), was applied and incubated for 1 h at room temperature. The slides were washed and mounted with fluorescence mounting medium containing DAPI and observed with confocal laser microscope. All images were analyzed using NIH Image J to assess the extent of implant-mediated cellular responses.

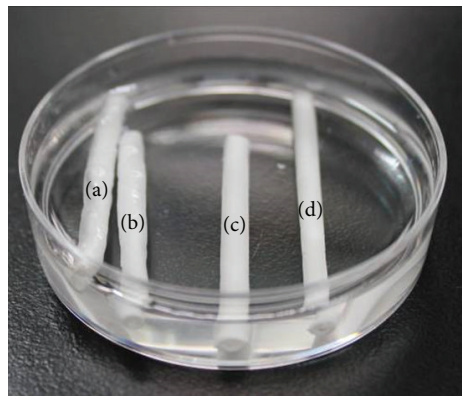

Figure 1: Tubular scaffolds (2 mm inner diameter) made of PCL and PCL/PTMC electrospun micro- and nanofibers. (a): PCL; (b): PCL/PTMC (3 : 1); (c): PCL/PTMC (1 : 1); and (d): PCL/PTMC (1 : 3).

2.5. Statistical Analysis. All quantitative results were obtained from five samples for analysis. Data were expressed as mean ± SD, and groups were compared using one-way ANOVA. Differences were considered statistically significant when $P < 0.05$.

3. Results and Discussion

3.1. Characterization of Electrospun PCL/PTMC Scaffold. Figure 1 showed 2 mm inner diameter tubular scaffold made of PCL and PCL/PTMC electrospun micro- and nanofibers. The wall thickness of PCL, PCL/PTMC (3 : 1), PCL/PTMC (1 : 1), and PCL/PTMC (1 : 1) scaffolds was 634 ± 47 μm, 615 ± 39 μm, 532 ± 27 μm, and 431 ± 18 μm, respectively. The cross section morphologies of the electrospun PCL and PCL/PTMC tubular scaffold were shown in Figure 2 by SEM. The scaffolds made of PCL, PCL/PTMC (3 : 1), and PCL/PTMC (1 : 1) were a random mix of micro- and nanofibers, which could be manufactured with a good reproducibility. The porosity of the tubular scaffolds decreased significantly with the increasing content of PTMC. Fiber fusion was found in PCL/PTMC (1 : 1) tubular scaffold (Figure 2(c)). When the content of PTMC was raised to 75%, the fibers were almost fused completely (Figure 2(d)).

The FT-IR spectra of PCL, PTMC, and electrospun PCL/PTMC fibers were shown in Figure 3. The spectrum of PCL was similar to the spectrum of PTMC (Figures 3(a) and 3(e)) because of the similarity of chemical structures of the two principle components. In PCL/PTMC blend fibers, these peaks were also found and changed slightly. Moreover, it could be observed that, with the increasing content of PTMC, the relative strength of peaks 1295, 1243, and 1192 cm^{-1} of PCL decreased. Almost no changes in the positions of these peaks were noted (Figures 3(b), 3(c), and 3(d)). This may be explained as the molecular interaction between PCL

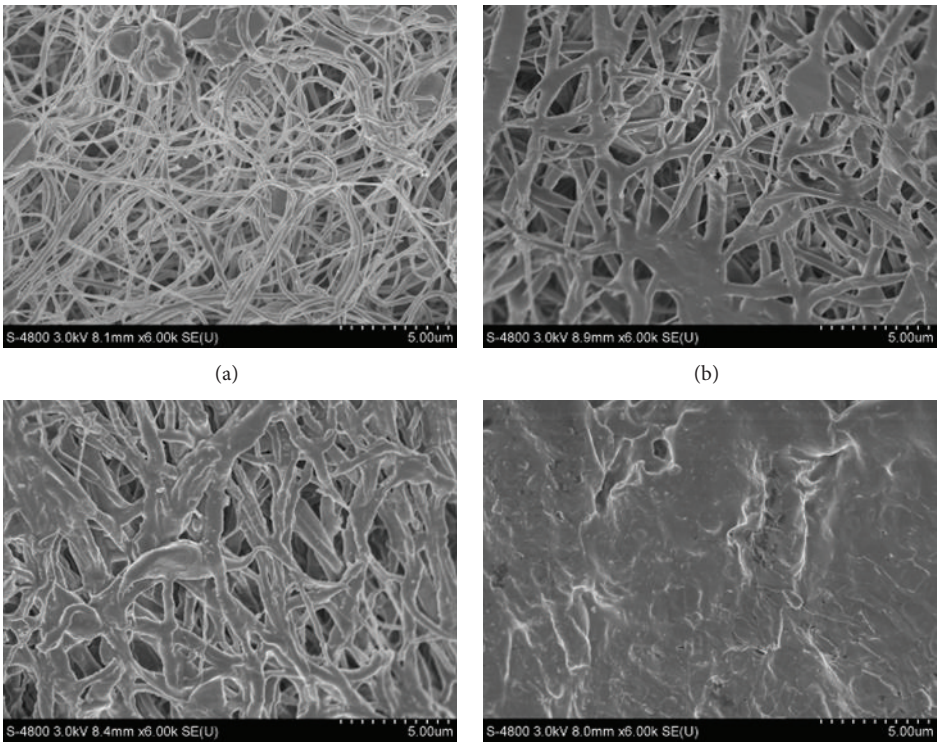

FIGURE 2: SEM showed the cross section morphological characters of electrospun PCL and PCL/PTMC tubular scaffolds. (a): PCL; (b): PCL/PTMC (3 : 1); (c): PCL/PTMC (1 : 1); and (d): PCL/PTMC (1 : 3).

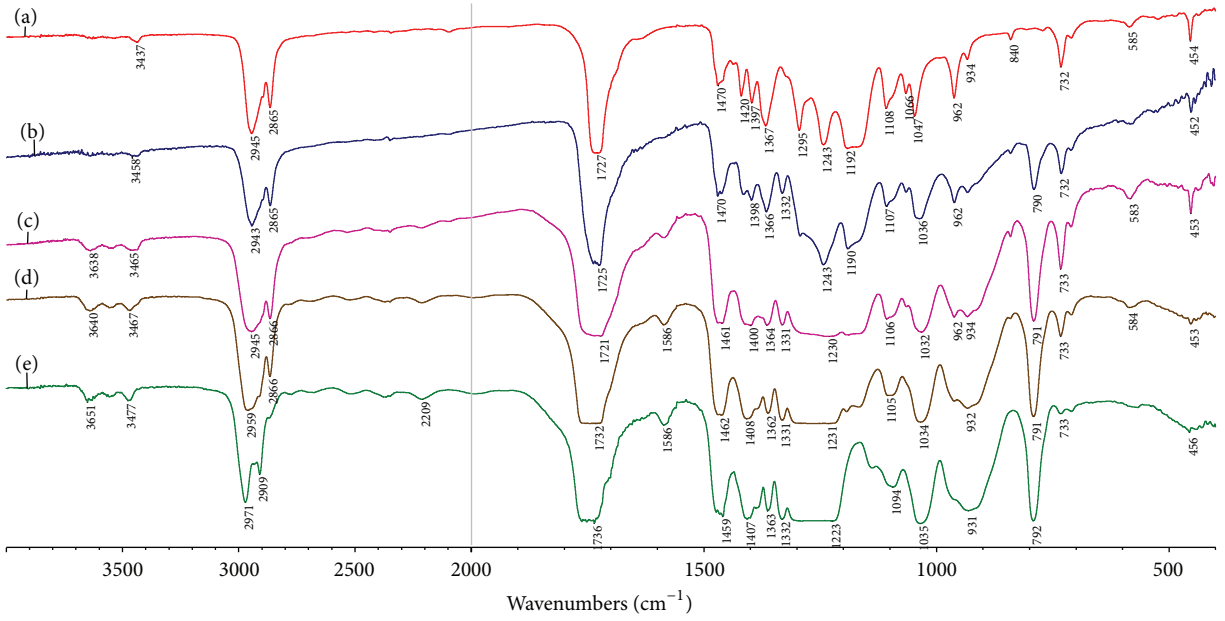

FIGURE 3: The FT-IR spectra of PCL, PTMC, and electrospun PCL/PTMC scaffolds. (a): PCL; (b): PCL/PTMC (3 : 1); (c): PCL/PTMC (1 : 1); (d): PCL/PTMC (1 : 3); and (e): PTMC.

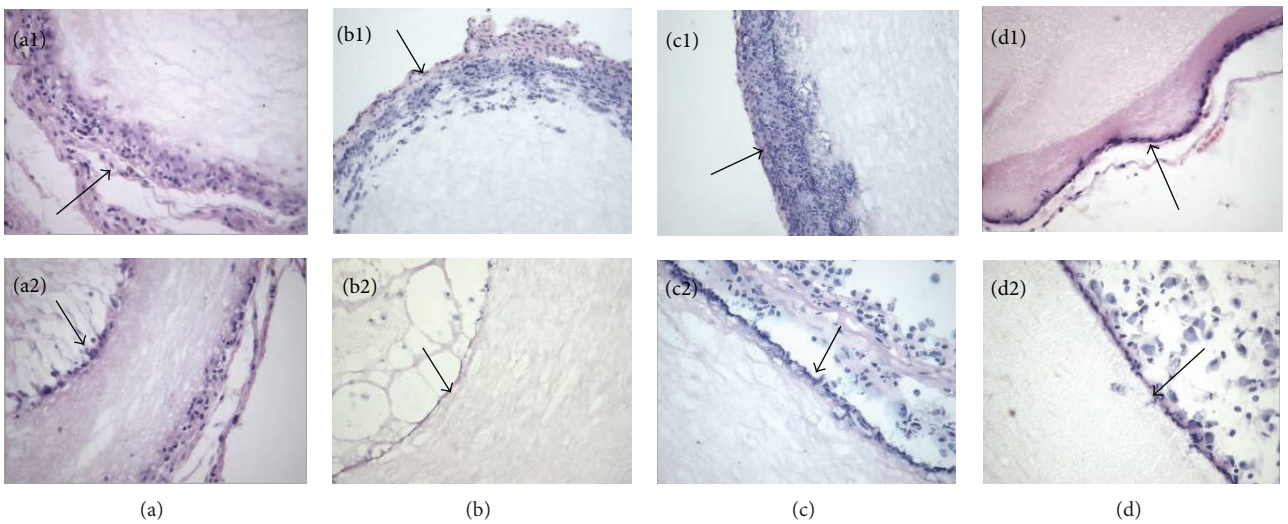

Figure 4: Histological aspect of cross sections of PCL and PCL/PTMC tubular scaffolds implanted for 1 month stained by HE. (a1)~(d1): Arrow indicated the adventitia of the tubular scaffolds; (a2)~(d2): arrow indicated the intima of the tubular scaffolds; (a1), (a2): PCL; (b1), (b2): PCL/PTMC (3 : 1); (c1), (c2): PCL/PTMC (1 : 1); and (d1), (d2): PCL/PTMC (1 : 3).

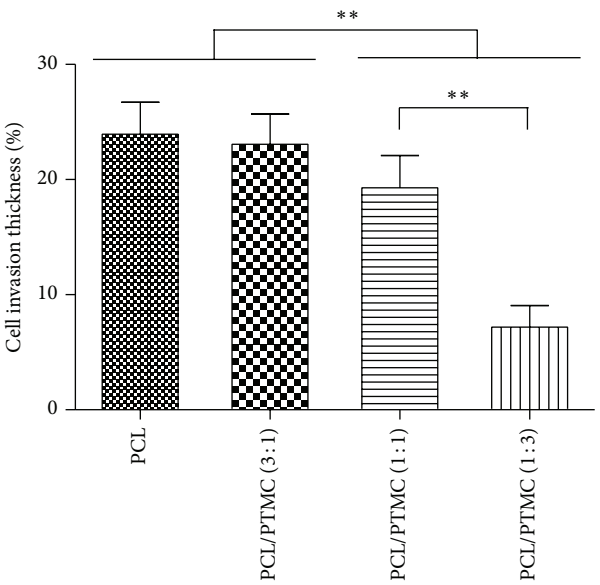

Figure 5: The cellular invasion in PCL and PCL/PTMC tubular scaffolds wall over 1 month ($^{**}P < 0.01$).

and PTMC is weak, because there are no chemical active groups (such as –OH and $–NH_2$) in the structure of either PCL or PTMC that would create a hydrogen bond forming environment.

3.2. The Degradation of Tubular Scaffold in Subcutaneous Space of Mice. PCL undergoes a two-stage degradation process: first, the nonenzymatic random hydrolytic cleavage of ester groups, which caused a decrease in molecular weight, and second, when the molecular weight was reduced to 3000 or less the polymer is completely resorbed and degraded via an intracellular mechanism [8]. Histological evaluation showed that the average thickness of PCL tubular graft wall remained constant during the experiment time. There were no notable changes in the fiber morphology of explanted grafts (Figure 4(a1)). Because the degradation of PCL compared to many other resorbable polymers is slow. The homopolymer PCL has a total degradation of 2~4 years (depending of the starting molecular weight of the device or implant) [13, 14].

The degradation process of PTMC is quite different from PCL, which degraded via surface erosion involving cellular-mediated processes without a change in molecular weight [15]. In our study, different level of degradation was found in various PCL/PTMC specimens after one month of implantation, as confirmed by histology. With the increase of concentration of PTMC, degradation speed also increased (Figures 4(b1), 4(c1), and 4(d1)). A fast decrease in thickness was observed in the PCL/PTMC (1 : 3) tubular scaffold. This decrease in thickness of tubular scaffold is not uniform, so that the outside diameter forms a concave uneven surface (Figure 4(d1)).

3.3. Tissue Response of Tubular Scaffold in Subcutaneous Space of Mice. A long term success of a biodegradable vascular graft must depend on proper regeneration of the vessel wall. Histological evaluation showed a series of events ensued after surgical implantation of the tubular scaffolds in the subcutaneous tissue. The main histopathologic changes were characterized by the arrival and infiltrate of acute inflammatory cells, monocytes/macrophages, lymphocytes, and fibroblasts in graft wall and an accumulation of wound fluid in graft lumen (Figure 4). After 4 weeks of implantation, the micro- and nanofiber structure and porosity of the PCL tubular scaffold allowed for infiltration of autologous cells. At the periphery of the graft, giant cells were present. But, there

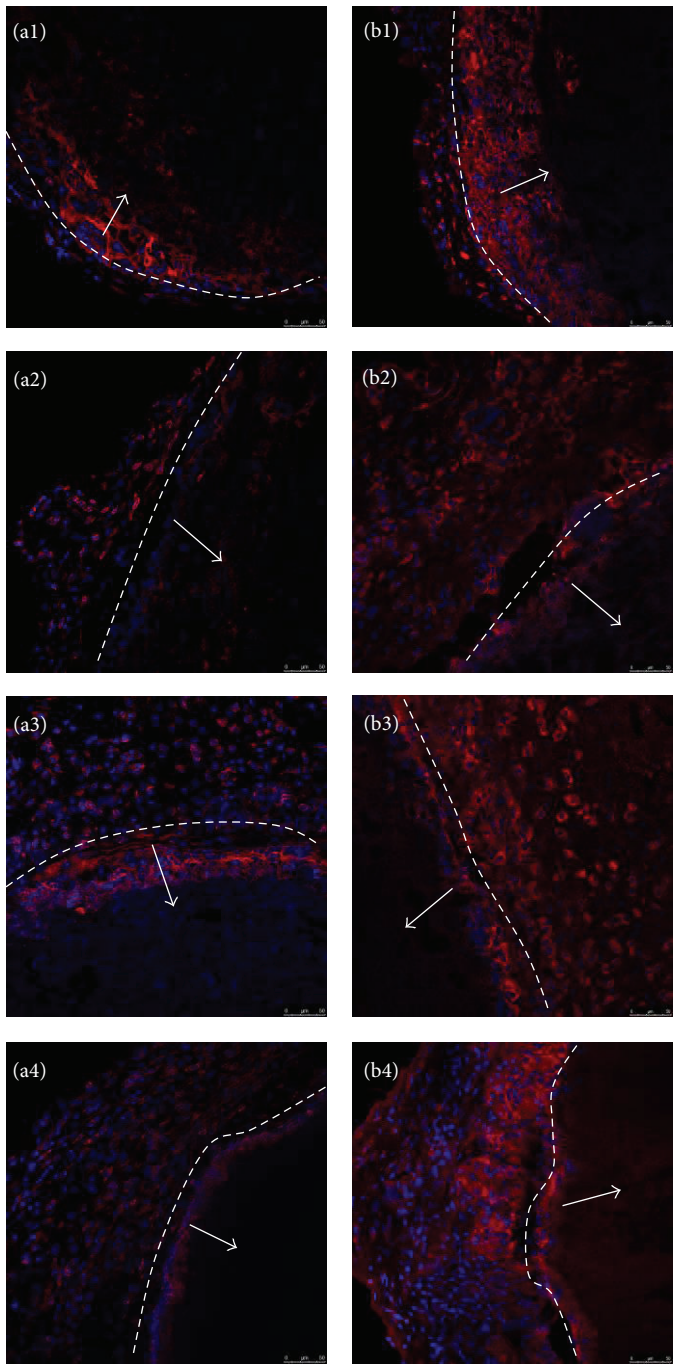

Figure 6: CLSM observation of CD11b+ and CD68+ cells accumulating in the tissue around PCL and different PCL/PTMC tubular scaffolds (3 : 1, 1 : 1, and 1 : 3) implanted for 1 month. Dotted line indicated the boundary of scaffold material and tissue. Arrow indicated the scaffold material. (a1)~(a4): CD11b+ cells; (b1)~(b4): CD68+ cells; (a1), (b1): PCL; (a2), (b2): PCL/PTMC (3 : 1); (a3), (b3): PCL/PTMC (1 : 1); and (a4), (b4): PCL/PTMC (1 : 3).

were no obvious fibrous capsules formed. This dense cellular population advances over the 4 weeks to 23.94 ± 2.76% of the graft's wall thickness (Figure 4(a1)). In graft lumen, there were a small number of cells in effusion (Figure 4(a2)). Similar histopathologic changes were found in PCL/PTMC (3 : 1) group and the cellular invasion ratio was 23.06 ± 2.62% (Figures 4(b1) and 4(b2)). Compared with PCL and PCL/PTMC (3 : 1) group, there were decreased cellar infiltration in the scaffold wall and increased macrophages and inflammatory cell in the lumen of the scaffold in PCL/PTMC (1 : 1) group (Figures 4(c1) and 4(c2)). The cellular invasion ratio was 19.29 ± 2.80% of the graft's wall

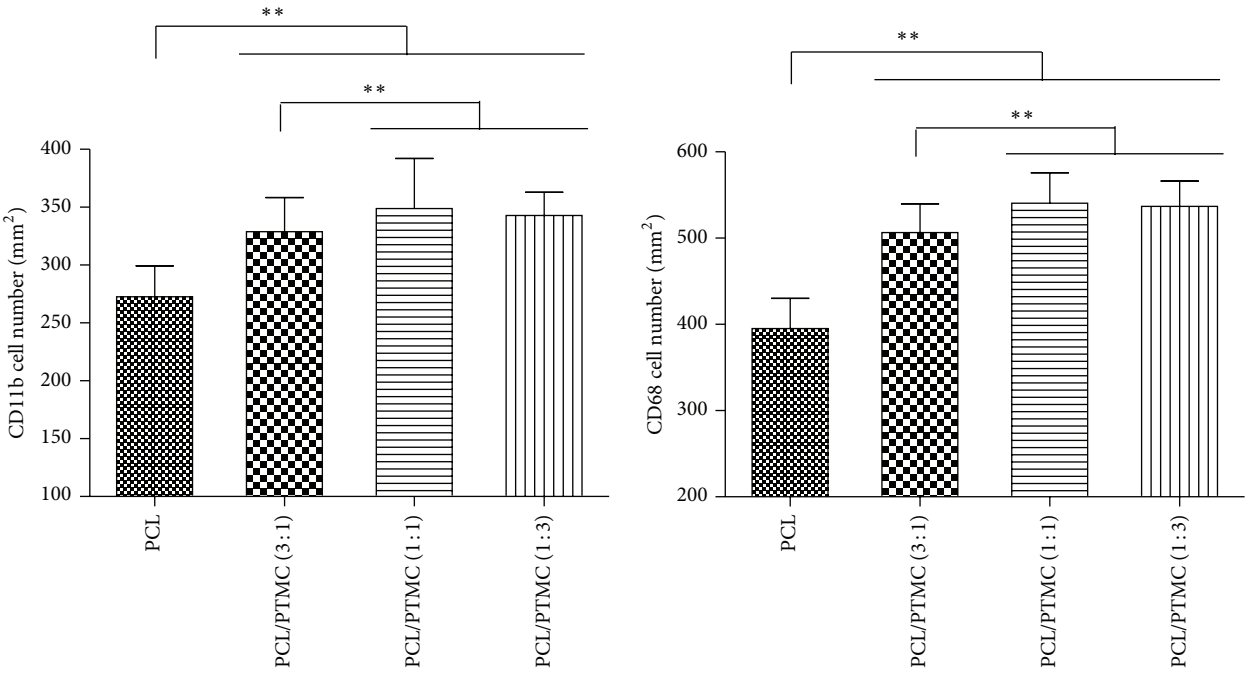

Figure 7: Quantitative analysis of CD11b+ and CD68+ cells accumulating in the tissue around PCL and different PCL/PTMC tubular scaffolds (3 : 1, 1 : 1, and 1 : 3) implanted for 4 weeks ($^{**}P < 0.01$).

thickness. In PCL/PTMC (1 : 3) group, the cellular population was sparse in the graft wall and the cellular invasion ratio was 7.19 ± 1.86%. The macrophages cluster and rapidly form a foreign body reaction with giant cells around the graft and inflammatory cells also were found in lumen (Figures 4(d1) and 4(d2)). The extent of the dense cellular infiltrate coming from the adventitia and made of fibroblasts and macrophages has been quantified (Figure 5).

3.4. Immunofluorescence Analyses of Inflammatory Cell Recruitment and Macrophages in the Foreign Body Reaction. To determine the cell types in the biomaterial implantation site, CD11b+ and CD68+ cells were detected by immunofluorescence analyses in this study. It was found that PCL tubular scaffold wall and implantation site contained CD11b+ inflammatory cells and CD68+ macrophages after 4-week implantation (Figures 6(a1) and 6(b1)). The number of CD11b+ inflammatory cells was 273 ± 27/mm^2 and the number of CD68+ cells was 395 ± 35/mm^2. In PCL/PTMC tubular scaffolds, with the increase of concentration of PTMC, there were increased CD11b+ inflammatory cells and CD68+ cells in the biomaterial implantation site after 4 weeks (Figures 6(a2~a4) and 6(b2~b4)). The number of CD11b+ and CD68+ cells in different groups had been quantified in Figure 7.

Chronic inflammation develops as inflammatory stimuli persist at the implant site with macrophages representing the driving force in perpetuating immune responses [16]. Macrophages also play a critical role in wound healing and tissue regeneration. Phagocytosis of wound debris, release of enzymes important for tissue reorganization and of cytokines, and growth factors inducing migration and proliferation of fibroblasts are mediated by macrophages and constitute the initial steps toward effective tissue regeneration [17]. In our study, the histological and immunofluorescence evaluation showed that the continuous degradation of PCL/PTMC scaffolds induced a stronger macrophage-mediated foreign body reaction than PCL scaffold. Therefore, the degradation of PCL/PTMC scaffolds may be in favor of the tissue regeneration in graft.

4. Conclusion

In this study, electrospun PCL/PTMC scaffolds were prepared with different blend ratios. With the increase of concentration of PTMC, the morphological feature and degradation speed of PCL/PTMC scaffold also changed. The histological and immunofluorescence evaluation showed that the continuous degradation of PCL/PTMC scaffolds induced a lasted macrophage-mediated foreign body reaction, which could be in favor of the tissue regeneration in graft. These results presented in this study demonstrated that electrospun PCL/PTMC scaffold material could be an excellent candidate for vascular tissue engineering.

Conflict of Interests

The authors declare that there is no conflict of interests regarding the publication of this paper.

Acknowledgments

This work was financially supported by Tianjin Municipal Natural Science Foundation (12JCYBJC19400) and the Doctoral Fund of Logistics University of CAPF (WYJ201103).

References

[1] S. A. Sell, M. J. McClure, K. Garg, P. S. Wolfe, and G. L. Bowlin, "Electrospinning of collagen/biopolymers for regenerative medicine and cardiovascular tissue engineering," *Advanced Drug Delivery Reviews*, vol. 61, no. 12, pp. 1007–1019, 2009.

[2] M. J. McClure, S. A. Sell, D. G. Simpson, B. H. Walpoth, and G. L. Bowlin, "A three-layered electrospun matrix to mimic native arterial architecture using polycaprolactone, elastin, and collagen: a preliminary study," *Acta Biomaterialia*, vol. 6, no. 7, pp. 2422–2433, 2010.

[3] H. Wu, J. Fan, C.-C. Chu, and J. Wu, "Electrospinning of small diameter 3-D nanofibrous tubular scaffolds with controllable nanofiber orientations for vascular grafts," *Journal of Materials Science: Materials in Medicine*, vol. 21, no. 12, pp. 3207–3215, 2010.

[4] L. Ye, X. Wu, Q. Mu et al., "Heparin-conjugated PCL scaffolds fabricated by electrospinning and loaded with fibroblast growth factor 2," *Journal of Biomaterials Science, Polymer Edition*, vol. 22, no. 1–3, pp. 389–406, 2011.

[5] S. de Valence, J.-C. Tille, D. Mugnai et al., "Long term performance of polycaprolactone vascular grafts in a rat abdominal aorta replacement model," *Biomaterials*, vol. 33, no. 1, pp. 38–47, 2012.

[6] Y. Song, M. M. Kamphuis, Z. Zhang et al., "Flexible and elastic porous poly(trimethylene carbonate) structures for use in vascular tissue engineering," *Acta Biomaterialia*, vol. 6, no. 4, pp. 1269–1277, 2010.

[7] B. L. Dargaville, C. Vaquette, F. Rasoul, J. J. Cooper-White, J. H. Campbell, and A. K. Whittaker, "Electrospinning and crosslinking of low-molecular-weight poly(trimethylene carbonate-co-l-lactide) as an elastomeric scaffold for vascular engineering," *Acta Biomaterialia*, vol. 9, no. 6, pp. 6885–6897, 2013.

[8] M. A. Woodruff and D. W. Hutmacher, "The return of a forgotten polymer—polycaprolactone in the 21st century," *Progress in Polymer Science*, vol. 35, no. 10, pp. 1217–1256, 2010.

[9] Z. Zhang, R. Kuijer, S. K. Bulstra, D. W. Grijpma, and J. Feijen, "The in vivo and in vitro degradation behavior of poly(trimethylene carbonate)," *Biomaterials*, vol. 27, no. 9, pp. 1741–1748, 2006.

[10] T. Fabre, M. Schappacher, R. Bareille et al., "Study of a (trimethylenecarbonate-co-ε-caprolactone) polymer-Part 2: in vitro cytocompatibility analysis and in vivo ED1 cell response of a new nerve guide," *Biomaterials*, vol. 22, no. 22, pp. 2951–2958, 2001.

[11] J. Han, C. J. Branford-White, and L.-M. Zhu, "Preparation of poly(ε-caprolactone)/poly(trimethylene carbonate) blend nanofibers by electrospinning," *Carbohydrate Polymers*, vol. 79, no. 1, pp. 214–218, 2010.

[12] A. Nair, J. Shen, P. Lotfi, C.-Y. Ko, C. C. Zhang, and L. Tang, "Biomaterial implants mediate autologous stem cell recruitment in mice," *Acta Biomaterialia*, vol. 7, no. 11, pp. 3887–3895, 2011.

[13] J. C. Middleton and A. J. Tipton, "Synthetic biodegradable polymers as orthopedic devices," *Biomaterials*, vol. 21, no. 23, pp. 2335–2346, 2000.

[14] P. A. Gunatillake and R. Adhikari, "Biodegradable synthetic polymers for tissue engineering," *European Cells and Materials*, vol. 5, pp. 1–16, 2003.

[15] A. P. Pêgo, M. J. A. van Luyn, L. A. Brouwer et al., "In vivo behavior of poly(1,3-trimethylene carbonate) and copolymers of 1,3-trimethylene carbonate with D,L-lactide or ε-caprolactone: degradation and tissue response," *Journal of Biomedical Materials Research A*, vol. 67, no. 3, pp. 1044–1054, 2003.

[16] J. A. Hamilton, "Nondisposable materials, chronic inflammation, and adjuvant action," *Journal of Leukocyte Biology*, vol. 73, no. 6, pp. 702–712, 2003.

[17] S. Franz, S. Rammelt, D. Scharnweber, and J. C. Simon, "Immune responses to implants—a review of the implications for the design of immunomodulatory biomaterials," *Biomaterials*, vol. 32, no. 28, pp. 6692–6709, 2011.